Rev.Adv.Mater.Sci. 15(2007) 79-86

PROBING BURIED INTERFACES BY SIMULTANEOUS COMBINATION OF X-RAY DIFFRACTION (SXRD) AND HARD X-RAY PHOTOELECTRON SPECTROSCOPY (HAXPES, UP TO 15KEV)

J.Rubio-Zuazo[1,2] and G.R.Castro[1,2]

[1]SpLine Spanish CRG Beamline at the ESRF, ESRF-BP 220-38043 Grenoble cedex-France
[2]Instituto de Ciencia de Materiales de Madrid-CSIC Cantoblanco E-28049 Madrid, Spain

Received: January 22, 2007

Abstract. In this contribution we present for the first time simultaneous combination of Surface X-Ray diffraction (SXRD) and Hard X-Ray photoelectron spectroscopy (HAXPES, photoelectrons with kinetic energy up to 15 KeV). Thanks to the simultaneous capability to detect the diffracted photons and the ejected photoelectrons, the developed experimental set-up offers a unique opportunity to obtain, on the same sample region and under identical experimental conditions, structural, electronic and chemical properties of the studied systems. Due to the high penetration depth of X-rays and the large escape depth of high energy photoelectrons (15 KeV kinetic energy) surfaces, bulk and buried interfaces are accessible in a non-destructive way. Its implementation at the Spanish CRG beamline (SpLine) at the European synchrotron radiation facility (ESRF) offers an exceptional tool capable to determine composition and structural profiles over a depth of several 10s of nanometers. A huge 2S+3D diffractometer house an ultra-high vacuum vessel equipped with a high energy analyzer. The set-up has been constructed that simultaneously fulfils the requirements for HAXPES and SXRD. Special effort has been devoted to develop a novel electron analyzer, capable of working at very high as well as low kinetic energies (from few eV up to 15 KeV). The first results are presented demonstrating the high efficiency of the proposed technique for structural, electronic and chemical properties determination.

1. INTRODUCTION

The advent of third generation synchrotron radiation sources gave rise to a variety of novel experimental techniques in the X-ray regime. For instance, the crystallographic study of surfaces became possible due to the high intensity X-ray beams provided by these sources giving birth the today well-known Surface X-Ray Diffraction (SXRD) [1,2]. Standard laboratory surface techniques, as X-ray photoelectron spectroscopy (XPS), also benefited from the high brilliance sources developing new alternatives as Angle-resolved XPS (ARPES) or spin resolved XPS [3]. However, the surface science is not only restricted to the study of clean surfaces, arising from the simple truncation of an infinite crystal, and surface reconstructions or superstructures. An important task on surface studies concerns with the physical and chemical modifications imposed by buried interfaces. Hard X-rays interact weakly with matter so that large penetration could be achieved enabling the crystallographic study of bulk materials and buried interfaces in the same way as surfaces,

Corresponding author: J.Rubio-Zuazo, e-mail: rubio@esrf.fr

by means of X-ray diffraction. However, buried interfaces are not accessible for the great majority of the techniques of surface physics, especially those based on electrons. The low electron inelastic-mean-free-path (IMFP) (few nm) in the solid at the energies used (between 40 and 2000 eV) is the responsible of their surface sensitivity.

Solid buried interfaces and chemical, compositional and electronic depth profiles are often analyzed by removing material while analyzing the properties of the surface [4]. The main disadvantage of this technique is the disintegration of the analyzed sample by the ion bombardment. Moreover, preferential sputtering usually occurs modifying the atomic environment compared to the real surroundings and hence inducing important uncertainties on the obtained results. A more efficient option consists on benefiting from the dramatic increase of the electron IMFP with the electron kinetic energy increase. This effect is indeed the one that gives its fundamental importance to the emerging XPS variant, the Hard X-ray photoelectron spectroscopy (HAXPES). Combining SXRD and HAXPES (up to 15 KeV), crystallographic, chemical and electronic information from buried interfaces and a correlation between surface and bulk properties will thus be accessible in a non-destructive way.

At the Spanish CRG SpLine beamline at the ESRF, a methodology based on hard X-rays as excitation source- for the study of surfaces and buried interfaces in a non-destructive way has been developed. Such a methodology, presented through this manuscript, concerns with the simultaneous combination of the recent emerging technique of Hard X-Ray Photoelectron Spectroscopy (HAXPES), up to 15 KeV photoelectron kinetic energy, and the Surface X-Ray Diffraction (SXRD) technique.

2. EXPERIMENTAL SET-UP

The experimental set-up developed at SpLine has been designed to fit the requirements for SXRD and HAXPES. Basically, see refs. [5] and [6] for specific information, the experimental set-up presented on this contribution is allocated on the hard edge (Branch B) of the bending magnet D25 at the ESRF covering a photon energy range between 5 and 45 KeV. A pseudo channel-cut double crystal monochromator [Si(111)] placed at ~30 m from the source monochromatizes the X-rays with a typical bandwidth of $\Delta\lambda/\lambda=1.5\cdot10^{-4}$. At the critical energy of 20.6 KeV a flux of 10^{13} photons/s flux can be

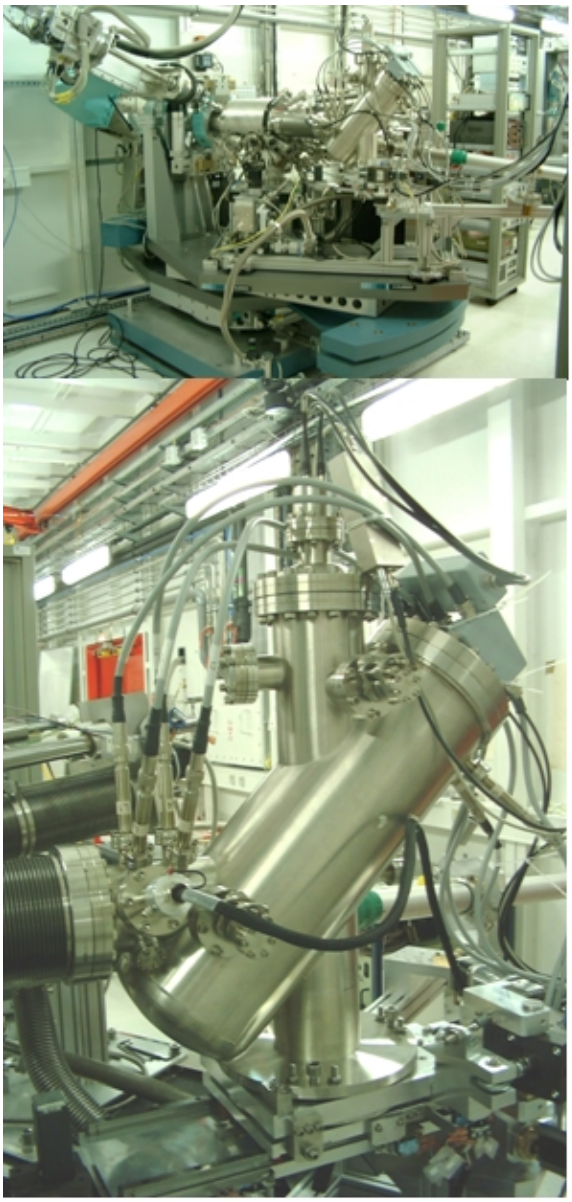

Fig. 1. (Up) Experimental set-up installed at the SpLine CRG beamline at the ESRF. A vacuum vessel equipped with a specially designed mini-LEED, an ion bombardment gun, an electron gun, evaporators, precision leak valves, a UV-discharge lamp, a mass spectrometer, an Helium cryostat, a sample transfer system and a high kinetic electrostatic analyzer is mounted on a robust 2S+3D diffractometer. Surface X-ray diffraction and Hard X-ray PES could be performed simultaneously using the same excitation source. (Down) Picture of the CSA300 electrostatic energy analyzer. It accounts with an internal and external radius of 32 mm and 130 mm respectively. The distance between the lens image and the detector (channeltron) is 300 mm. The approximated weight is 30 kg. Hence, the CSA is characterized by its reduced dimension and weight.

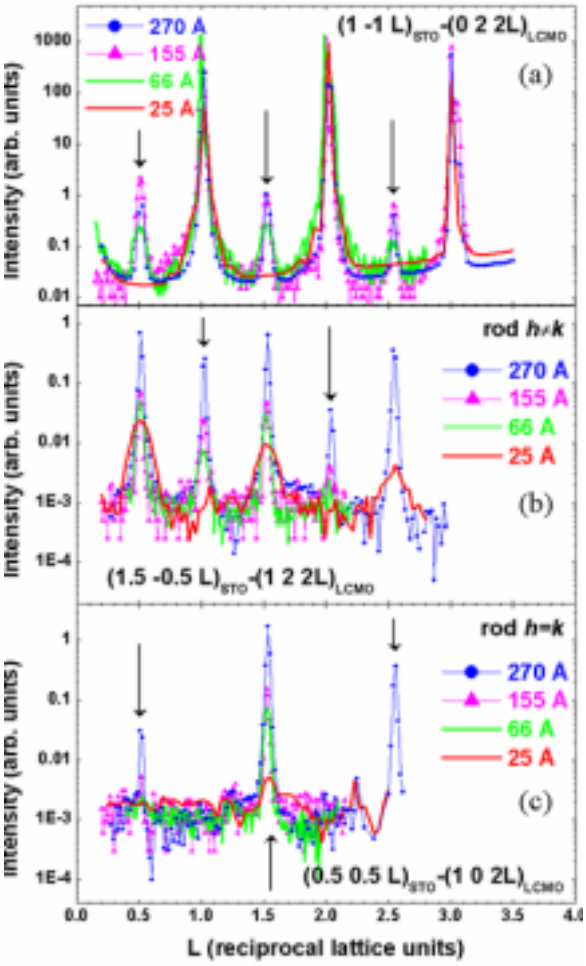

Fig. 2. Representative SXRD measurements on $La_{0.7}Ca_{0.3}MnO_3/SrTiO_3$ thin films. Out-of-plane scans for a 24, 66, 155, and 270 Å film are shown along (a) (1 –1 *l*)-CTR, (b) (1.5 –0.5 *l*)-rod, and (c) (0.5 – 0.5 *l*)-rod directions. Half integer *l*-peaks in (a) and integer *l*-peaks in (b) are missing for the 24 Å film. No intensity was obtained in (c) for the 24 Å film.

achieved that is well adapted for the HAXPES and SXRD requirements. A spot size of <1mm^2 is attained by sagittal cylindrical bending of the second monochromator crystal and by cylindrical bending of the mirror placed after the monochromator, which is also used for harmonic rejection. A high resolution channel-cut [Si(311), Si(333) and Si(400)] post-monochromator is foreseen in case a better resolution in the HAXPES measurements is necessary. The experimental set-up, shown in Fig. 1, consists on a UHV vessel mounted on a robust 2S+3D diffractometer and equipped with a especially developed electrostatic analyzer able to analyze photoelectrons up to 15 KeV kinetic energy.

The UHV vessel is specifically adapted for SXRD and HAXPES. It incorporates a specially designed mini-LEED, an ion bombardment gun, an electron gun, evaporators, precision leak valves, a UV-discharge lamp, a mass spectrometer, an Helium cryostat and a sample transfer system that allows the possibility of doing SXRD and HAXPES experiments during growth deposition or different sample treatment. The diffractometer is operated on horizontal geometry, i.e., sample surface mounted vertically, taking advantage of the synchrotron horizontal polarization and the wide angular divergence from the focused bending magnet source. Finally, the electron analyzer [7] is a sector of a cylindrical mirror analyzer with a five elements retarding lens system, which is designed for a small geometrical size compared to mostly used hemispherical analyzers. The sample-lens distance is maximized to 50 mm, allowing the simultaneous accomplishment of photoemission and diffraction experiments and enabling also in-situ measurements (deposition, ion sputtering, etc). The electron analyzer covers a wide energy range, from few eV to 15 KeV so low and high kinetic energy electrons could be analyzed enabling the correlation between surface and bulk (buried interface).

3. SURFACE X-RAY DIFFRACTION (SXRD)

SXRD is a valuable technique that provides very precise information on surface and interface atomic arrangement of crystalline structures [1,2]. By varying the angle of incidence, the penetration of the evanescent wave into the material can be controlled allowing the analysis of surfaces and buried interfaces. SXRD is a powerful tool for surface structural characterization of properties such as atomic structure, roughness, relaxation and reconstruction. It is also well adapted to analyze in deep the atomic structure, the registry, the misfit relaxation, the growth mode and the morphology of adsorbate/substrate interfaces. Additionally it is not subject to charge effects as in the case of electron diffraction.

In the case of an infinite three-dimensional crystal the diffraction effect is restricted to different points lattice in reciprocal space given by the three Laue's equations. When the crystal is truncated, the loss of periodicity along the direction perpen-

dicular to the surface leads to a relaxation of one of the Laue's conditions. The diffraction is still sharply peaked in both directions parallel to the surface while in the out-of-plane direction the intensity becomes a continuum (CTR). The reciprocal space is therefore made of rods in the direction normal to the surface which extends over a volume inversely proportional to the size of the crystal.

In the case of a reconstructed surface, the atoms move parallel to the surface producing a new bidimensional symmetry and lattice. Hence, rods are found at fractional order values of $h_{substrate}$ and $k_{substrate}$ where the bulk does not contribute to the scattered amplitude. It will be only determined by the contribution from a quasi-2D crystal of finite thickness. The rod modulation period is directly associated with the layer thickness and the modulation amplitude is related to the magnitude of the atomic displacements normal to the surface.

Fig. 2 shows an example of SXRD measurements on $La_{0.7}Ca_{0.3}MnO_3/SrTiO_3(001)$ thin films. A CTR and two ROD´s representative of the recorded database (based on 50 different reflections CTR's and ROD's) are presented for four films with thicknesses 2.4, 6.6, 14.4, and 27 nm. Both CTRs and RODs show intensity maximal at half integer L values due to that the c parameter (out-of-plane) of the bulk manganite ($La_{0.7}Ca_{0.3}MnO_3$) is twice the lattice parameter of the $SrTiO_3$ (STO substrate) Also due to the $\sqrt{2}\times\sqrt{2}R45$ superstructure reflections with *a,b* (in-plane) half integer cubic indices (referred to the STO lattice) are also present. Clearly we distinguish different behavior for the 2.4 nm film compared to the thicker films. Remarkable is the disappearance of the half integer peaks in the CTR's scans and of the integer peaks in the ROD's scans with *H≠K* for the 2.4 nm film. In the ROD's scans *H=K* (superstructure crystallographic axis) no peaks were found for the 2.4 nm film. Based on the extinction conditions we are able to determine the crystallographic space group for each film, which results to be Ibam or I4/mcm for the 2.4 nm film and Pbnm (bulk space group) for the 6.6, 14.4, and 27 nm film [8,9]. Table 1 recovers the main results from the detailed intensity study. The atomic positions are obtained with high accuracy by fitting the calculated intensity from a proposed structure to the measured intensities. In the present case the intensity analysis also revealed the presence of the 2.4 nm film structure at the interface of the other films, concluding that the change on crystal structure, compared to bulk, present at the films-substrate interface is the main responsible of the anomalous magnetic properties of doped manganate thin films.

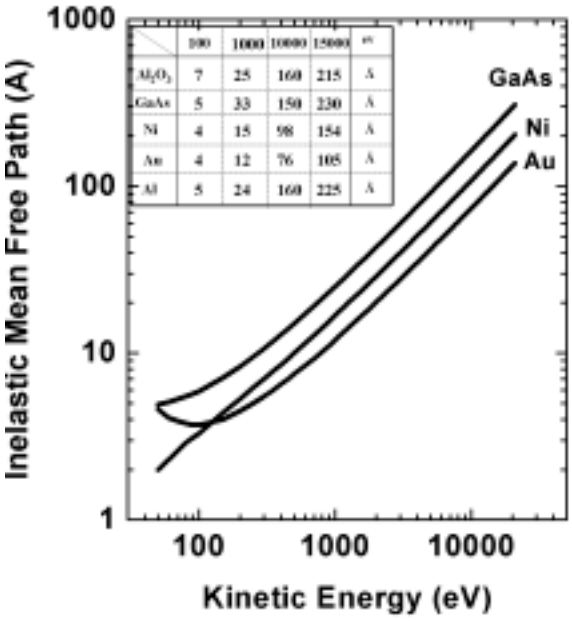

Fig. 3. Curve for the electron mean free path as a function of the electron kinetic energy. The electron mean free path range between 4 and 100 Å as a function of material and electron energy for energies up to 5 KeV. Thus, the observation of photo-emitted electrons at the mentioned energies intrinsically emphasizes the surface contribution. When the electron kinetic energy is shifted to high energies, i.e., 15 KeV, it could be guessed that inelastic mean free path about 230 Å could be achieved.

4. HARD X-RAY PHOTOELECTRON SPECTROSCOPY (HAXPES)

The photoemission spectroscopy consists on the detection of the emitted electrons of a sample due to the interaction of the electromagnetic radiation. Depending on the used excitation energy it is possible to distinguish between UPS (UV Photoelectron Spectroscopy) and XPS (X-ray Photoelectron Spectroscopy). In general, their application has been limited to the investigation of surface phenomena, by using energies between 40 and 2000 eV, due to the low electron inelastic-mean-free-path (IMFP) achieved at the energies used. However, the IMFP in solid materials at 10 keV reaches ap-

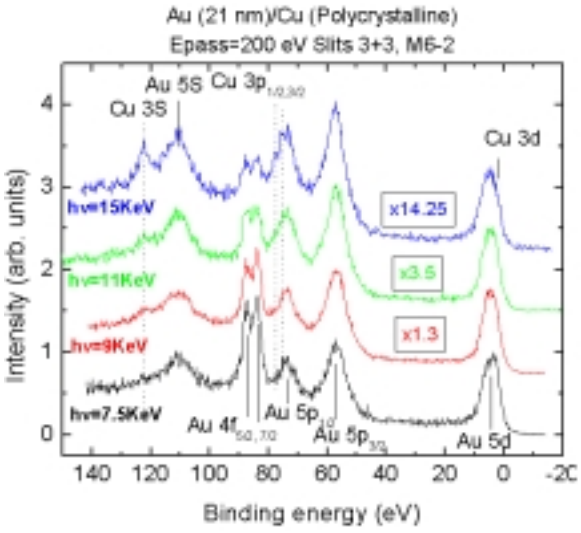

Fig. 4. Representative spectra of HAXPES from a polycrystalline copper sample covered by a 210 Å thick gold layer. The near valence band region is shown for different excitation photon energies. The spectra are normalized onto the Au 5d peak heights. It could be clearly observed that only when the highest kinetic energy is used (15 KeV) the copper electrons can travel through the 210 Å thick gold layer. This spectra demonstrates the excellent capability of HAXPES to probe buried interfaces.

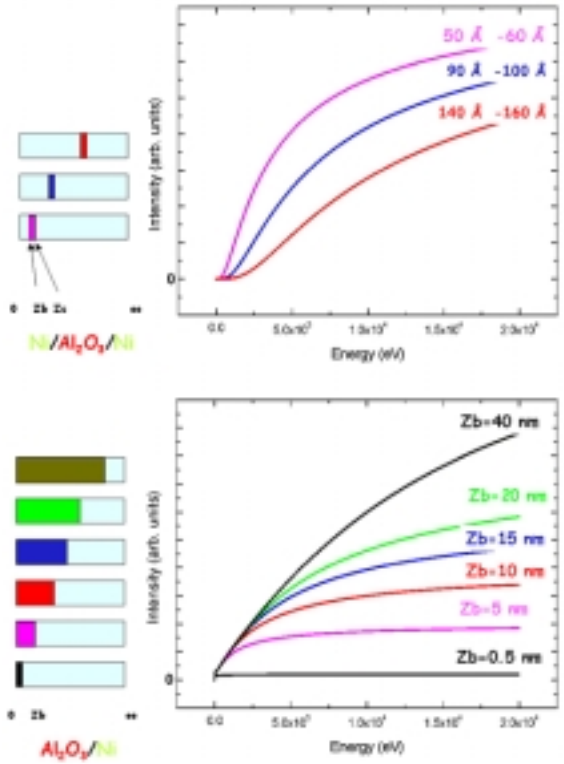

Fig. 5. Simulation of the photoemission intensity as a function of the photoelectron kinetic energy for two different composition depth profiles: overlayer [$n(z)$=1 for 0<Z<Zb and $n(z)$=0 for Z>Zb] the intensity increases due to the increase of amount of material contributing to the signal up to the kinetic energy where λ>Zb for which the intensity remains constant. In the case of a buried interface [$n(z)$=0 for 0<z<Zb and Z>Zc, and $n(z)$=1 for Zb<Z<Zc] no intensity is measured up to a kinetic energy is reached where Zb<λ<Zc. Then the intensity follows the same behavior as in the overlayer case.

proximately 10 nm and at 15keV can reach about 25 nm as estimated from the extrapolation of the TTP-2M equation, [10,11] shown in Fig. 3. This effect is indeed the one that gives its fundamental importance to the hard X-ray photoemission spectroscopy. Although for many years a restlessness interest to develop this technique has existed, two factors have fundamentally prevented their implementation: The low flux of conventional X-ray sources (X-ray tubes) which cannot handle the decrease of the photoionization cross-section with the excitation energy increase and the non-existence of commercial analyzers operating above 5 KeV. Nowadays, with the 3rd generation high brilliance synchrotron sources which provide enough intensity to compensate the photoionization cross-section decrease, many laboratories around the world are starting research programs concerning the implementation of HAXPES [12]. Some companies are developing electron analyzers able to detect high kinetic energy electrons but their maximum energy is limited to 12 KeV. Today, our Cylindrical Sector Analyzer [7], developed in cooperation with the company FOCUS GmbH, Germany, is the unique commercial analyzer able to operate at electron kinetic energies up to 15KeV.

Fig. 4, shows representative spectra of HAXPES from a polycrystalline copper sample covered by a 21 nm thick gold layer. The near valence band region is shown for different excitation photon energies. The spectra is normalized onto

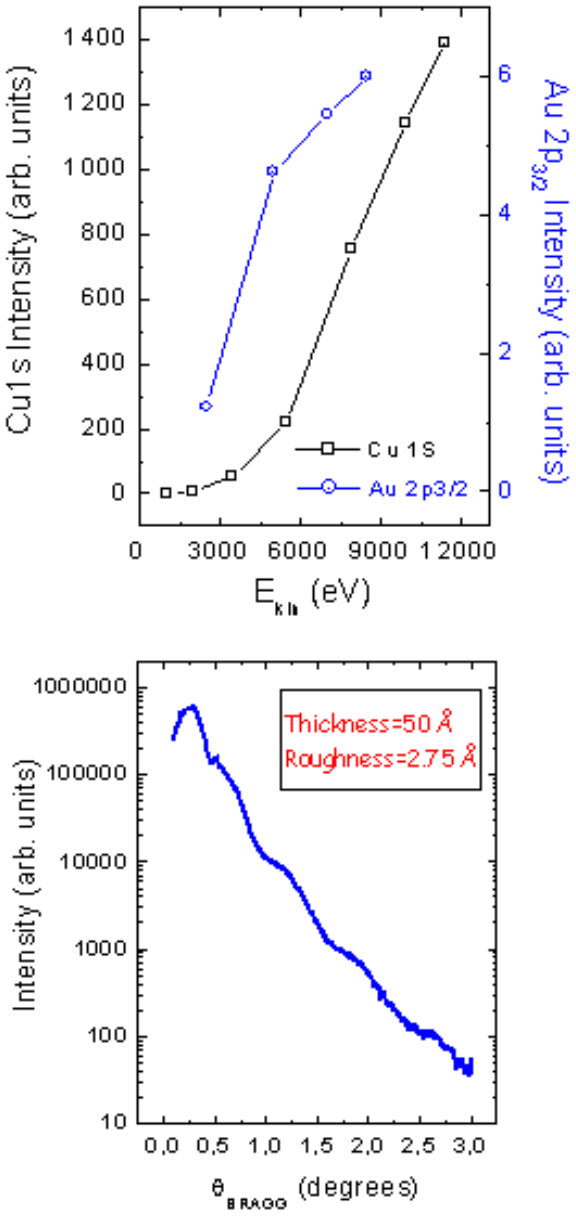

Fig. 6. (Up) Cu 1s and Au 2p3/2 photoemission intensity, normalized with the parameters mentioned in the text, as a function of the photoelectron kinetic energy for a polycrystalline copper sample covered by 50 Å thick gold layer. The Cu 1s signal appears at a kinetic energy of ~2 KeV, i.e., where $\lambda(E_{kin})$ ~Au layer thickness, and rises for higher kinetic energies. The Au $2p_{3/2}$ rises from the beginning and initiates to saturate at the same kinetic energy where the Cu signal starts to rise. (Down) Corresponding low angle X-ray diffraction measurement where it could be clearly observed the Kiessig fringes arising from the overlayer finite thickness.

the Au 5d peak heights. It could be clearly observed that only at high kinetic energies (15 KeV) the emitted electrons from the copper could travel through the 21 nm thick gold layer and hence being detected. The Cu 3s and Cu $3p_{1/2,3/2}$ are clearly resolved when the photoelectron kinetic energy reaches 15 KeV. These measurements confirm that HAXPES allows the determination of electronic properties and chemical composition of bulk and buried interfaces.

5. SIMULTANEOUS COMBINATION OF SXRD AND HAXPES: COMPOSITIONAL DEPTH PROFILE ANALYSIS

In our experimental set-up the same X-rays are used simultaneously for SXRD and HAXPES ensuring that the complementary information is obtained from the same sample region and under identical sample conditions, i.e., same vacuum conditions and without moving the sample position or changing the excitation source characteristic. The simultaneous combination of both techniques is of special relevance when performing in-situ measurements, i.e., during growth process, thermal heating, following the structural and electronic modification through the temperature transition, *etc.*

Non-destructive composition depth profile analysis is a representative application of the simultaneous combination of SXRD and HAXPES. The depth profile is obtained by following the intensity of the photoelectrons from a constituent element of the substrate and/or overlayer film by changing the escape depth of the photoelectrons, i.e., changing the energy of the incident X-rays and hence the kinetic energy of the photoelectrons. The intensity of photoelectrons from the element is given by [13],

$$I_0(E_{kin}) = Af(E_{h\nu})\sigma_0(E_{h\nu})\Gamma(E_{kin})P(E_{kin},\theta)\times \int_0^z n(z)\exp\left(-\frac{z}{\lambda\cos\theta}\right)dz, \quad (1)$$

where A is the ratio between the area irradiated with X-rays and the area seen by the analyzer, $f(E_{h\nu})$ is the intensity of the incident X-rays, $\sigma_0(E_{h\nu})$ is the photoionization cross-section, $\Gamma(E_{kin})$ is the detector transmission function which depends on the kinetic energy of the photoelectrons, $P(E_{kin},\theta)$ is the correction factor for the angular anisotropy of the photoemission process which depends on the detection configuration, λ is the effective attenuation

Table 1. Main relevant parameters obtained from the diffraction intensities analysis for the 24 Å and 270 Å film of $La_{0.7}Ca_{0.3}MnO_3/SrTiO_3(001)$.

	24 Å film	270 Å film
Symmetry space group	$D_{4h}^{18} - 14/mcm$, $D_{2h}^{26} - Ibam$	$D_{2h}^{16} - Pbnm$
Out-of-plane lattice parameter	c=7.73 Å	c=7.73 Å
Film thickness	24 Å	270 Å
Mixed domains	[*hkl*]-[*khl*]	[*hkl*]-[*khl*]
Film terminating layer	Single MnO_2	Single MnO_2
Substrate termination	Single TiO_2	Single TiO_2
Substrate film interface	TiO_2-$La_{2/3}Ca_{1/3}{}^{O}$	TiO_2-$La_{2/3}Ca_{1/3}{}^{O}$
Film roughness	4 Å	6 Å

length of the photoelectrons and θ denotes the angle between collection direction and the surface normal. Therefore, by proper normalization, Eq. (1), it is possible to extract from the experimental data the concentration profile *n(z)*.

Fig. 5 shows a simulation of the photoemission intensity as a function of the photoelectron kinetic energy for two different composition depth profiles, overlayer and buried interface. It could be clearly observed that for an overlayer [$n(z)$=1 for 0<Z<Zb and $n(z)$=0 for Z>Zb] the intensity increases due to the increase of amount of material contributing to the signal up to the kinetic energy where λ>Zb for which the intensity remains constant. In the case of a buried interface [$n(z)$=0 for 0<Z<Zb and Z>Zc, and $n(z)$=1 for Zb<Z<Zc] no intensity is measured up to a kinetic energy is reached where Zb<λ<Zc. Then the intensity follows the same behavior as in the overlayer case. It should be stressed that in order to obtain a precise depth profile, the transmission function of the analyzer should be calibrated and the photoionization cross-section and effective attenuation lengths should be tabulated for the kinetic energies involved. Up to now, limited data for $\sigma_0(E_{h\nu})$ and $\lambda(E_{kin})$ is available in the photon energy range for which the kinetic energy of the emitted photoelectrons ranges under the HAXPES scope. The depth profile is hence obtained by performing a fit to the measured curves (I vs E_{kin}) by means of Eq. (1). For a preliminary study we have assumed a $Z^4E(h\nu)^{-3.5}$ dependency for the cross-section on the excitation photon energy. The dependence of the effective attenuation length on photoelectron kinetic energy has been derived from the TTP-2M equation. [10]. A precise knowledge of the overlayer thickness at the sample region studied is fundamental for an accurate determination of the depth profile. Low angle X-ray reflectivity provides the exact thickness of the deposited film. It should be stressed that thanks to the simultaneous combination of both techniques, the obtained thickness belongs to the sample area analyzed by HAXPES. Fig. 6 (up) represents the measured intensity for the Cu 1s and Au $2p_{3/2}$ shells, normalized wit the above assumptions, for a polycrystalline copper sample covered by a 5.0 nm thick gold layer. Fig. 6 down illustrates the corresponding low angle X-ray diffraction measurement where it could be clearly observed the Kiessig fringes arising from the overlayer finite thickness. The photoemission intensity dependence on the photoelectron kinetic energy behaves as expected. The Cu 1s signal appears at a kinetic energy of ~2 KeV, i.e., where $\lambda(E_{kin})$ ~Au layer thickness, and rises for higher kinetic energies. The Au $2p_{3/2}$ rises from the beginning and initiates to saturate at the same kinetic energy where the Cu signal starts to rise. The depth profile has not been performed due to the lack of precision on the photoionization cross-sections and effective attenuation lengths. In future work, after the cross-sections and effective attenuation lengths tabulation, we will analyze depth profiles based on the presented methodology.

6. CONCLUSIONS

The developed experimental set-up offers a unique opportunity to obtain, on a same sample and un-

der identical experimental conditions, simultaneous information about the electronic properties, geometric structure and chemical composition of bulk, buried interfaces and surfaces. The implementation of the Hard X-ray Photoelectron spectroscopy will open a direct way to correlate surface and bulk properties and in combination with Surface X-ray Diffraction will open a new research field. The first obtained HAXPES spectra have been presented demonstrating the excellent capability to probe buried interfaces. A methodology to perform depth profile analysis has been described based on the variation of the electron escape depth with the kinetic energy increase.

ACKNOWLEDGEMENTS

We would like to express our gratitude to the SpLine staff for their valuable help in carrying out this research. Special thanks are addressed to M. Escher and M. Merkel and to all the staff of the Focus GmbH for the excellent cooperation in the development of the electron analyzer. Financial support for this research was provided through MEC, former MCYT (Spanish ministry of Education and Science) grants No. FAP-2001-2166 and No. MAT1999-0241-C01.

References

[1] I.K.Robinson, In: *Handbook of Synchrotron Radiation Vol. 3*, ed. by Brown and Moncton (Elsevier Science Publisher, Amsterdam, 1991), p. 221.

[2] R. Feidenhans // *Surf. Sci. Reports* **10** (1989) 105.

[3] *Electron Spectroscopy for Surface Analysis*, ed. by H.Ibach (Springer-Verlag, Berlin Heidelberg, 1984).

[4] H.J.Mathieu, In: *Thin film and depth profile analysis*, ed. by H.Oechsner (Springer-Verlag, Berlin Heidelberg, 1984), p. 39.

[5] G.R.Castro // *J. Synchrotron Rad* **5** (1998) 657.

[6] J.Rubio-Zuazo and G.R.Castro // *Nucl. Instr, Meth A* **547** (2005) 64.

[7] J.Rubio-Zuazo and G.R.Castro // *Rev. Sci. Instr*, in press.

[8] A. de Andrés, J. Rubio, G.R. Castro, S. Taboada, J.L. Martínez and J.M. Colino // *Appl Phys. Lett* **83** (2003) 713.

[9] J. Rubio-Zuazo, A. de Andrés, S. Taboada, C. Prieto, J. L. Martínez and G. R. Castro // *Phys. B* **357** (2005) 159.

[10] S.Tanuma, C.J.Powell and D.R.Penn // *Surf. Interf. Anal.* **25** (1997) 25.

[11] M.P.Seah and W.A.Dench // *Surf. Interf. Anal* **1** (1979) 2.

[12] *Proceedings of the Workshop on Hard X-ray Photoelectron Spectroscopy* // *Nucl. Instr. Meth. Phys. Resch. A* **547** (2005).

[13] S. Hüfner, In: *Photoelectron Spectroscopy* (Springer Verlag, 1994).